DAMPING REDUCTION FACTORS FOR MAXIMUM ROTATED SPECTRA FOR ANALYSIS OF BASE-ISOLATED STRUCTURES

Cicek K.[1] and Erkus B.[2]

[1]*Res. Assist., Dept. of Civil Eng., Istanbul Technical University, Istanbul*
[2]*Assist. Prof. Dr., Dept. of Civil Eng., Istanbul Technical University, Istanbul*
Email: bariserkus@itu.edu.tr

ABSTRACT:

This paper investigates damping reduction factors for equivalent single-degree-of-freedom analysis of base isolated structures with maximum rotated spectral acceleration spectra. Current literature on DRFs for the modification of a given response spectrum in the analysis of base isolated structures for higher damping is mostly based on the energy dissipation in the major axes of the structure, which is compatible with geometric mean intensity measure. On the other hand, some of the recent structural codes such as ASCE 7-16 uses maximum rotated design spectrum for estimation of effective displacement demands of the isolators. Literature on DRFs for maximum rotated spectra has not been reported. In this study, first an idealized model of a base-isolated structure is established. In this model, the isolation layer is represented as a single isolator with bilinear behavior and biaxial coupling, and the superstructure is modeled with single mass with bidirectional degrees of freedom. No viscous damping added to the isolation layer. Various values of yield levels, stiffness values are considered to establish a group of structures. Second, a large set of historical ground motion data is selected, and several levels of seismicity are considered by amplitude scaling the ground motions. Nonlinear time-history analyses are performed for all isolator models and scaled seismic ground motions. Maximum isolator displacements are estimated using three approaches: (a) applying each component of the ground motions independently in a unidirectional fashion, (b) bidirectional analysis with both components of the ground motion and using geometric mean measure of the displacements considering the biaxial interaction (c) same as previous with maximum rotated measure. Effective periods and damping values are estimated from the maximum displacements. DRFs are estimated by finding the ratio of these values to the displacements of a corresponding linear system, where estimated effective period and 5% viscous damping are used and unidirectional and bidirectional analyses are performed to be compatible with the isolation model results. Least-squares criteria is used to fit power-law-based curves to the simulation data for three types of DRF. These curves are compared to the DRFs provided by major structural codes and some well-known estimates available in the literature. It is found that directional aspects of ground motion has minor affect on the DRFs, while use of hysteretic damping through nonlinear analysis instead of viscous damping with a linear system has moderate affect on the DRFs.

KEYWORDS: damping reduction factor, response spectra, intensity measure, maximum rotated, geometric mean, base-isolation.

1. INTRODUCTION

Seismic base isolation is an effective method for protection of structures against earthquakes, and number of base isolated buildings has increased significantly in the past decade. This trend is also valid for Turkey. Turkish Ministry of Health requires large hospitals located in high seismic regions to have base isolation. New Turkish code for seismic design of buildings (TBEC-18 2018) includes a section for seismic base isolation.

Design of structures with seismic base isolation has some challenges. The design and the production of the isolators has to be completed in a short period of time to be inline with the construction schedule. Most of the time, it is not possible to conduct sophisticated analysis to verify the isolator design and simplified and approximate methods have to be employed. It is, therefore, essential to understand how accurate these simplified methods from the points of view of both safety and economy.

One of the approximate methods that is used frequently in the design of isolation systems of the base-isolated structures is equivalent single-degree-of-freedom (SDOF) method. In this method, a crucial step is to

estimate an equivalent damping that corresponds to the energy dissipated by the hysteretic behavior of isolators, which is generally significantly larger than the inherent energy dissipated by the structure. Therefore, acceleration spectrum, which is used for design or analyses and which is generally available for a 5% viscous damping, has to be adjusted. This factor is known as *damping reduction factor* (DRF). For practicing engineers, this factor is provided by structural codes, which are in fact based on research available in the literature.

Estimation of DRFs are mostly based on linear analyses with viscous damping, where time-history analyses of linear SDOF systems with various values viscous damping ratios (ξ) and periods (T) for a large group of seismic ground motion data are conducted. Ratio of the response of these SDOF systems to a 5% damped SDOF system with the same period gives the DRFs. Generally, a curve-fitting procedure is applied to obtain a DRF function of only the damping ratio ξ (e.g. Ashour 1987; Tolis and Faccioli 1999; Ramirez *et al.* 2002; Priestley *et al.* 2007) or the damping ratio and the period ξ, T (e.g. Newmark and Hall 1982; Wu and Hanson 1989; Naeim and Kircher 2001; Ramirez *et al.* 2002; Lin and Chang 2004; Arakawa 2012). There are also seismic-hazard-based or soil conditions studies that estimate acceleration spectra for different values of viscous damping, which uses the first method (Rezaeian *et al.* 2012; Sheikh *et al.* 2013; Akkar *et al.* 2014). Various proposed functions for DRFs are compared in literature (Lin *et al.* 2005; Cardone *et al.* 2009; Lin *et al.* 2003).

Design of base isolated structures has certain characteristics that are not immediately compatible with the conventional definitions of DRFs. First of all, all of the available literature uses uni-directional analyses, while geometric mean (e.g. TBEC-18 2018) or maximum rotated (e.g. ASCE 7-16 2016) intensity measures are generally used in the design of base isolated structure. Second, conventional isolation systems such as friction pendulums and lead-rubber bearings have hysteretic energy dissipation, rather than viscous damping, and there is no literature on estimation of DRFs on using hysteretic energy dissipation. Finally, there is biaxial interaction between the components of the isolation shear forces. Estimation of DRFs that takes all these aspects of base isolation systems into account does not exist in the literature.

The main purpose of this study, is to investigate DRFs for base isolation design when a maximum rotated (MR) spectrum is used. The study uses a typical bilinear model for the nonlinear behavior of isolators, and biaxial interaction is included for bidirectional analyses. Properties of the bilinear model, *i.e.*, primary and secondary stiffness, yield strength are selected such that they reflect possible friction pendulum and lead rubber bearing properties. A large set of isolator models is generated by considering various values for each isolator property. Twenty one pairs of earthquake ground motion acceleration data are selected, where the magnitude of the earthquakes are in the order of 7. Two types of analyses are performed. In the first type, ground motion is applied unidirectional similar to conventional DRF analyses. In the second type, bidirectional analyses are performed. DRFs are estimated based on the unidirectional response from the first type of analyses and geometric mean and maximum rotated response from the second type. Effective periods are estimated from these displacements and corresponding isolator forces. A linear system is considered with the effective system estimated and 5% viscous damping. Analyses on this system are also performed in unidirectional and bidirectional fashion to be compatible with the isolation system model. Ratios of the maximum displacements are estimated to find the DRFs. Results are presented graphically and comparison to available values of DRFs is provided.

2. CURRENT LITERATURE ON DAMPING REDUCTION FACTORS

Table 1 concludes the review on the previous section with some of the equations and brief information of the belonging studies or codes. Figure 1 represents the graphical outcome and comparison of the DRF equations.

As can be seen from Figure 1. Japanese Code has the lowest DRFs. Eurocode 8 (2004), Akiyama (1985), Ashour (1987) and Kasai *et al.* (2003) have similar DRF values and they are similar to NCSE-02 (2002) and GJ50011-10 (2010) for damping ratios larger than 35%. Newmark and Hall (1982), CAL-SEIS-10 (2010), Tolis and Faccioli (1999) and IT-STR-08 (2008) are more conservative than the others.

3. THEORY

This section gives a brief review on the isolator modeling, effective damping and damping reduction factors.

Table 1. Damping reduction factors (DRFs)

Literature	Equation	Notes
Eurocode 8 (2004) and TBEC-18 (2018)	$\sqrt{\frac{10}{5+\xi}}$ *	See Bommer *et al.* (2000)
FEMA 440 (2005) and ASCE 7-16 (2016)	$\frac{4}{5.6-\ln(\xi)}$ *	
CALTRANS (CAL-SEIS-10 2010)	$\frac{1.5}{0.4\xi+1}+0.5$ *	See Kawashima and Aizawa (1986)
Japanese Code (JP-ISO-01 2001)	$\frac{1.5}{1+10\xi}$ **	
French and Spanish NCSE-02 (2002)	$(5/\xi)^{0.4}$ *	
Old Italian Code (IT-STR-08 2008)	$\sqrt[3]{\frac{7}{2+\xi}}$ *	New Italian Code uses Eurocode 8 (2004)
Chinese Code (GJ50011-10 2010)	$1+\frac{0.05-(\xi)}{0.06+1.4\xi}$ **	See Zhou *et al.* (2003)
Newmark and Hall (1969)	$1.309-0.194ln(\xi)$ *	
Akiyama (1985)	$\frac{1+3h_0+1.2\sqrt{h_0}}{1+3h+1.2\sqrt{h}}$ **	h_0: initial effective damping h: effective damping
Ashour (1987)	$\sqrt{\frac{0.05(1-e^{-\alpha\xi})}{\xi(1-e^{-0.05\alpha})}}$ **	$18<\alpha<65$. Suggested $\alpha=18$ for design.
Tolis and Faccioli (1999)	$\sqrt{\frac{15}{10+\xi}}$ *	
Kasai *et al.* (2003)	$\sqrt{\frac{1+25h_0}{1+25h}}$ **	h_0: initial effective damping h: effective damping
Lin and Chang (2004)	$1-\frac{aT^{0.3}}{(T+1)^{0.65}}$	$a=1.303+0.436ln\xi$ *

*: ξ is in terms of percentage, e.g. $\xi=30$ for a damping ratio of 0.30
**: ξ, h, h_0 are in terms of ratio, e.g. $\xi=0.30$ for a damping ratio of 0.30

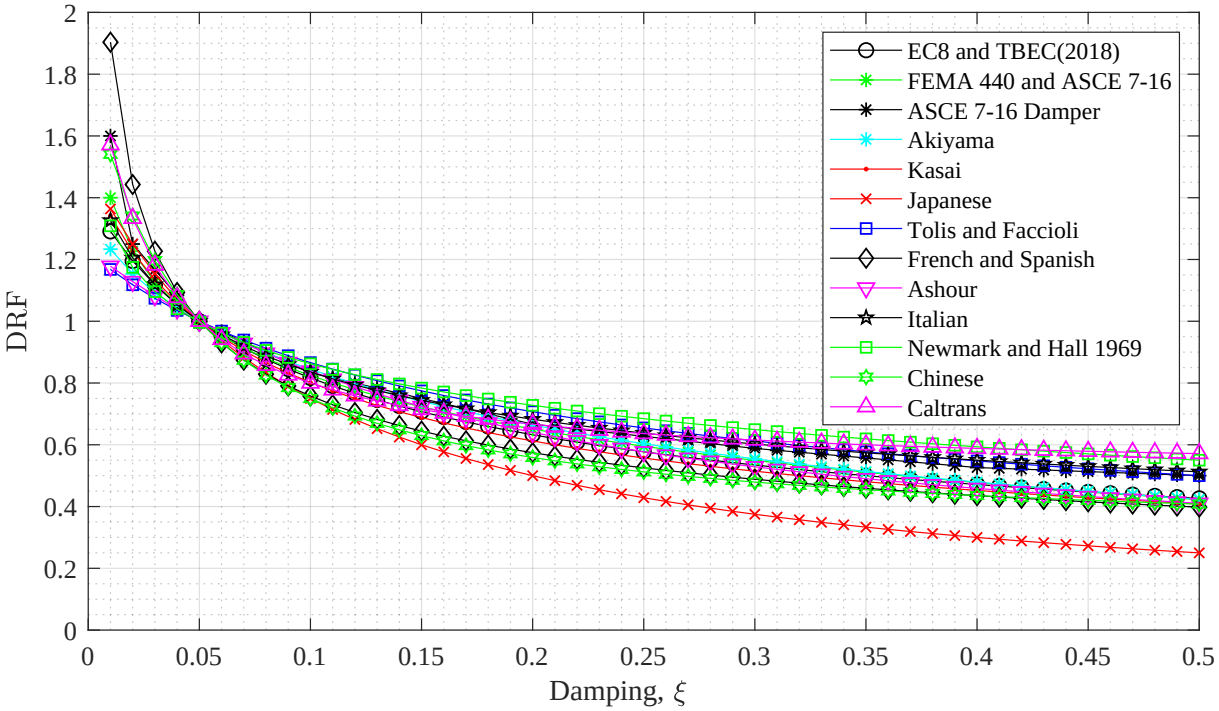

Figure 1. Comparison of the DRF formulations

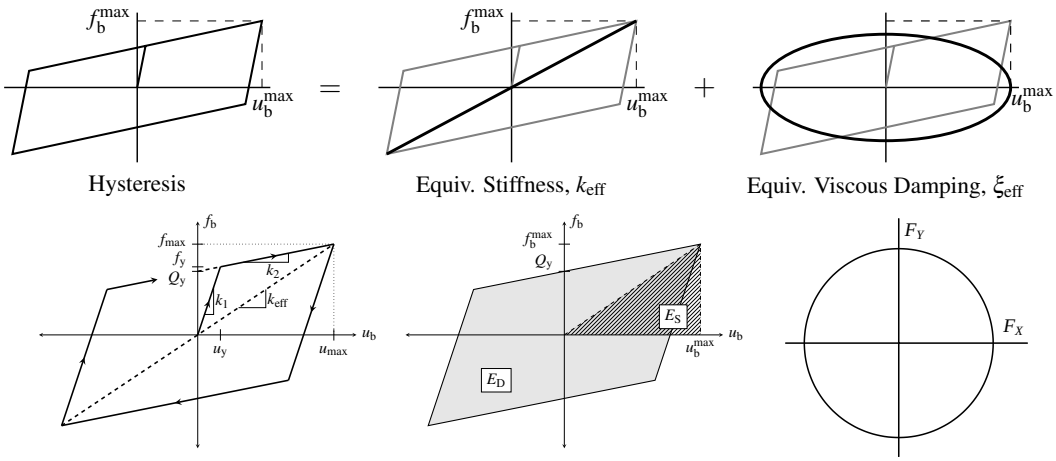

Figure 2. Equivalent damping, isolator model, energy terms and biaxial coupling yield surface

3.1. Nonlinear Modeling of Isolators

Typical bilinear element is used to model the behavior of seismic isolators (see Figure 2). Parameters that define the bilinear behavior are primary stiffness k_1, secondary stiffness k_2, and yield force f_{y}. In this study, biaxial coupling of the isolator shear forces (Figure 2) is also considered and implemented through the analysis software OpenSees (2008). The elastomeric bearing model of OpenSees, which uses a plasticity-based coupling model by Huang (2002), is used.

3.2. Equivalent Damping

Conventional definition of equivalent viscous damping is used. This definition is based on the assumption that hysteretic behavior of a nonlinear element is equivalent to superposition of a linear spring and a viscous damping as shown in Figure 2. Equivalent damping is estimated by

$$\xi = \frac{E_{\text{D}}}{4\pi E_{\text{S}}} \tag{1}$$

where E_{D} is the hysteretic energy dissipated by the nonlinear element in one cycle and E_{S} is the strain energy of the equivalent linear spring at the maximum displacement (Figure 2).

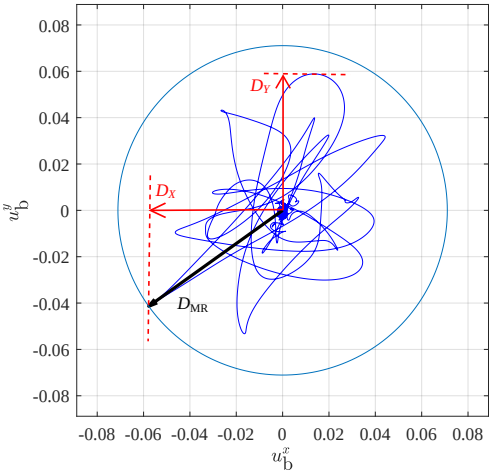

Figure 3. Displacements used for MR and GM measures

3.3. Uni- and Bi-Directional Displacement Demand Measures

For the estimation of DRFs, three types of measures of the isolator displacements are used.

ONE-DIR: This is simply the maximum uni-directional response of the isolator for a given ground motion data, D_X^{UNI} and D_Y^{UNI}. For a pair of historical ground motion data the isolator model is analyzed for the two horizontal components separately.

BI-DIR GM: This is a bi-directional measure of the isolator response, where geometric mean of the two horizontal displacement demands is estimated as follows:

$$D_{\text{GM}} = \sqrt{D_X^{\text{BI}} \times D_Y^{\text{BI}}} \tag{2}$$

where D_X^{BI} and D_Y^{BI} are maximum displacements of the isolator in the orthogonal horizontal directions when a bi-directional analysis is performed and bi-axial coupling of the isolator forces is considered (Figure 3). Note that for linear systems, $D^{\text{BI}} = D^{\text{UNI}}$ for both $X-$ and $Y-$directions

BI-DIR MR: This is a bi-directional measure of the isolator response, maximum resultant demand is estimated:

$$D_{\text{MR}} = \max(u_{xy}(t)), \qquad u_{xy}(t) = \sqrt{(u_x(t))^2 + (u_y(t))^2} \tag{3}$$

Table 2. Summary of the DRFs estimated

Name	Estimated Measures	Reference Demands
ONE-DIR LIN	$D_X^{\text{LIN, UNI}}$, $D_Y^{\text{LIN, UNI}}$ (using T_{eff}, ξ_{eq})	$D_X^{\text{LIN, UNI}}$, $D_Y^{\text{LIN, UNI}}$ (using T_{eff}, $\xi = 5\%$)
BI-DIR GM LIN	$D_{\text{GM}}^{\text{LIN, BI}}$ (using T_{eff}, ξ_{eq})	$D_{\text{GM}}^{\text{LIN, BI}}$ (using T_{eff}, $\xi = 5\%$)
BI-DIR MR LIN	$D_{\text{MR}}^{\text{LIN, BI}}$ (using T_{eff}, ξ_{eq})	$D_{\text{MR}}^{\text{LIN, BI}}$ (using T_{eff}, $\xi = 5\%$)
ONE-DIR NL	$D_X^{\text{NL, UNI}}$, $D_Y^{\text{NL, UNI}}$, T_{eff} and ξ_{eq}	$D_X^{\text{LIN, UNI}}$, $D_Y^{\text{LIN, UNI}}$ (using T_{eff}, $\xi = 5\%$)
BI-DIR GM NL	$D_{\text{GM}}^{\text{NL, BI}}$, T_{eff} and ξ_{eq}	$D_{\text{GM}}^{\text{LIN, BI}}$ (using T_{eff}, $\xi = 5\%$)
BI-DIR MR NL	$D_{\text{MR}}^{\text{NL, BI}}$, T_{eff} and ξ_{eq}	$D_{\text{MR}}^{\text{LIN, BI}}$ (using T_{eff}, $\xi = 5\%$)
BI-DIR (MR NL) / (GM LIN)	$D_{\text{MR}}^{\text{NL, BI}}$, T_{eff} and ξ_{eq}	$D_{\text{GM}}^{\text{LIN, BI}}$ (using T_{eff}, $\xi = 5\%$)
BI-DIR (GM NL) / (ONE DIR LIN)	$D_{\text{GM}}^{\text{NL, BI}}$, T_{eff} and ξ_{eq}	$(D_X + D_Y)^{\text{LIN, UNI}}/2$ (using T_{eff}, $\xi = 5\%$)
BI-DIR (MR NL) / (ONE DIR LIN)	$D_{\text{MR}}^{\text{NL, BI}}$, T_{eff} and ξ_{eq}	$(D_X + D_Y)^{\text{LIN, UNI}}/2$ (using T_{eff}, $\xi = 5\%$)

Similar to BI-DIR GM, bi-directional analysis is performed and bi-axial coupling is considered. The notation *MR* is used since this measure is compatible with maximum rotated spectra (Figure 3).

3.4. Estimation DRFs - Conventional Approach

In the conventional approach, maximum displacement of a linear SDOF system for a given period and viscous damping is divided by the displacement of a SDOF system with the same period and the reference viscous damping, which is generally 5% of the critical damping:

$$\beta = \frac{D^{\text{LIN}}(T, \xi)}{D^{\text{LIN}}(T, \xi = 5\%)} \tag{4}$$

3.5. Estimation of DRFs - Proposed Approach

In this study first, in addition to the conventional estimates of DRF, another method is proposed for estimation of DRFs, where two aspects of base-isolation systems are considered: (a) use of bi-directional displacement demand measures and (b) use of isolator nonlinear behavior for estimation of displacement (Table 2).

For the ONE-DIR NL estimate of DRF, uni-directional nonlinear analyses are performed, and maximum displacements and corresponding effective period and damping values are estimated for each direction separately. For these effective periods and 5% viscous damping linear analyses are performed and maximum displacements are obtained. DRFs are estimated by dividing the former maximum displacement to the latter maximum displacement. For the BI-DIR GM NL measure of DRF, geometric mean of the maximum displacements of the nonlinear system in the $X-$ and $Y-$directions are estimated. For this displacement, effective period and effective damping is estimated using the isolator properties k_1, k_2 and f_y. Then, linear analyses are performed for the estimated effective period and 5% viscous damping, and geometric mean of the maximum displacements is found. DRF is estimated by finding the ratio of the former to the latter. Similarly calculations are performed for the BI-DIR MR NL measure. These DRFs based on the bi-directional nonlinear analyses includes the effects of nonlinear behavior, but not the directional effects effectively since the denominator of the DRF is also a bi-directional quantity, and division may simply filter out the possible directional effects.

The BI-DIR (MR NL) / (GM LIN) estimate of the DRF is for the purpose of estimating isolator displacements using a structural code that utilizes geometric mean as the intensity measure for design spectrum. This is due to the fact that design isolator displacements should be based on the resultant displacements rather than $X-$ or $Y-$components or geometric mean of these components. This value of BI-DIR (MR NL) / (GM LIN) DRF is expected roughly 1.3~1.4 times the conventional DRF values. BI-DIR (GM NL) / (ONE DIR LIN) and BI-DIR (MR NL) / (ONE DIR LIN) are defined to investigate the effects of bi-directional analysis.

4. NUMERICAL SIMULATIONS

In this section first, the seismic ground motion database that is used in the estimation of DRFs is given. Second, verification of the analysis is provided for one set of isolator properties. Finally, DRF values and best-fit curves are shown graphically for uni-directional and bi-directional demand measures.

Table 3. Ground motion data set

PEER No.	Earthquake	Mag. (M)	R_{Rup} (km)
838	Landers,1992	7.28	34.86
882			26.84
900			23.62
1101	Kobe, 1995	6.9	11.34
1104			17.85
1121			27.77
1158	Kocaeli, 1999	7.51	13.6
1165			3.62
1166			30.73
1176			1.38
1602	Duzce, 1999	7.14	12.2
1605			6.58
1634	Manjil, 1990	7.37	75.58
1787	Hector Mine, 1999	7.13	10.35
3758	Landers,1992	7.28	36.93
5836	El Centro, 2010	7.2	28.53
6013			27.81
6886	Darfield, 2010	7.0	14.48
6952			18.73
6953			24.55
6960			13.64

Table 4. Parameter set used in the analysis

Parameter	Values
k_1	f_y/u_y
k_2	[0.07, 0.11, 0.15] k_1
f_y	[0.01, 0.03, 0.05, 0.07, 0.10] W
u_y	2.5 cm
m	17500 tons
EQ. Scaling	0.5, 1, 1.5, 2, 2.5

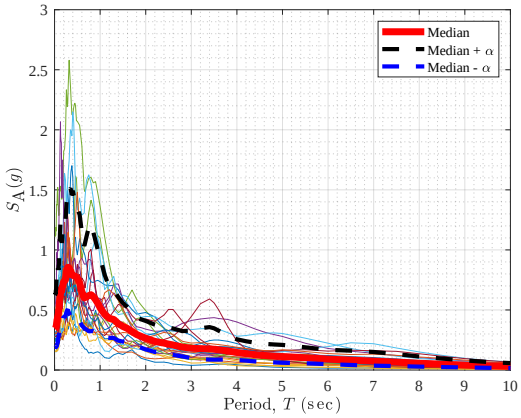

Figure 4. Pseudo acceleration GM spectra of the ground motion data set

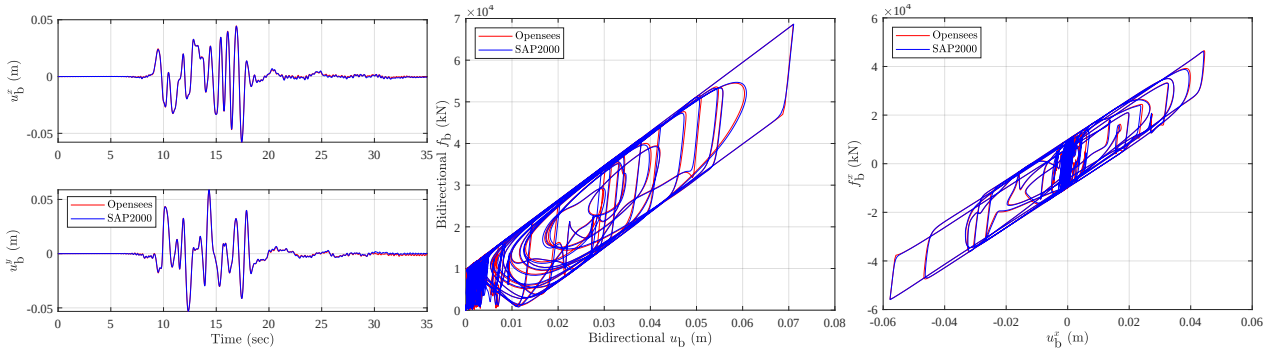

Figure 5. Verification of the OpenSees model with SAP2000

The historical ground motion data given in Table 3 is used in this study. Pseudo acceleration spectra of the data set is shown in Figure 4. In this study, OpenSees (2008) is used for the simulations. OpenSees models are verified with SAP2000 (2018) (Figure 5). The data set used in the analysis is summarized in Table 4. The analyses that resulted $D < 5$ cm are discarded. This set of isolator parameters results effective periods up to around 5.5 seconds and equivalent damping ratios of up to 50% (Figure 6).

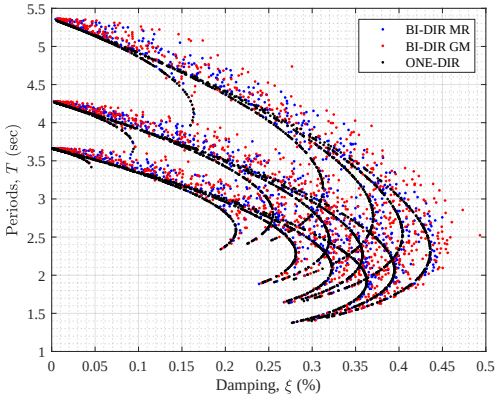

Figure 6. Range of effective periods and equivalent damping values

4.1. Uni-directional Analyses

Figure 7 shows the results of the uni-directional analyses. Figure 7a and 7b shows the results when conventional linear analyses and proposed nonlinear analyses, respectively, are performed for the estimation of DRFs. The fitted functions and their parameters are provided in Section 4.4.. Figure 7c compares the linear analyses results with the formulas available in the literature. Figure 7d compares the DRFs estimated from linear and nonlinear analyses.

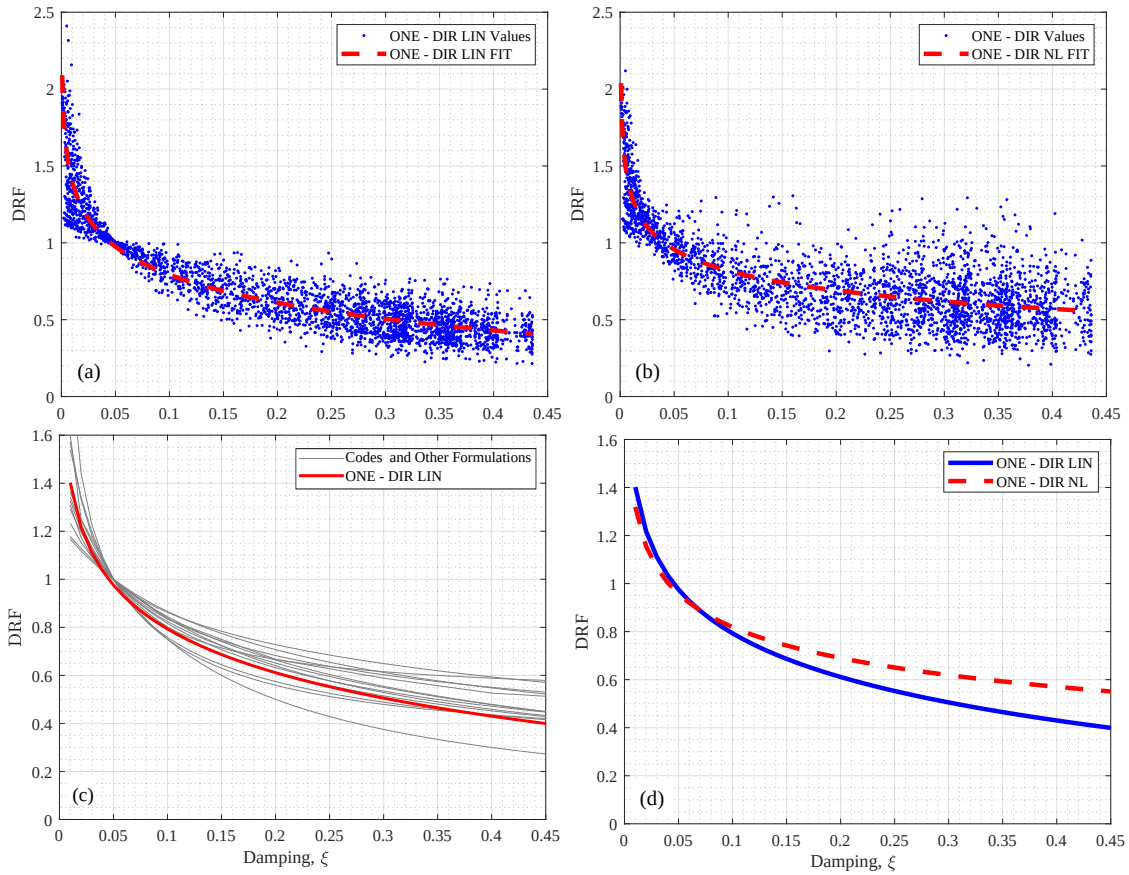

Figure 7. Results for the uni-directional analyses (a) linear DRF, (b) nonlinear DRF, (c) linear vs available literature and (d) linear DRF vs nonlinear DRF

It is observed from these results that there is significant scatter around the fitted curves. The scatter is larger for the nonlinear analyses. These results shows that for certain isolator parameters and earthquakes, use of DRFs can significantly miscalculate the isolator demands. Comparison of the curve estimated from conventional linear analyses to the available literature shows some of the structural codes have conservative estimates of DRFs. This may be associated with the seismic ground motion selected and intentional conservatism added by the researchers (e.g. Ramirez *et al.* 2002). The comparison of DRFs from nonlinear analyses to linear analyses shows that equivalent SDOF approach tends to underestimate nonlinear the displacement demands for hysteretic systems and the difference becomes more evident for the larger values of equivalent damping. This difference is further elaborated in Section 4.2.

4.2. Bi-directional Analyses

Figure 8 shows the results of the bi-directional analyses for the MR measure of the displacements. Figure 8a and 8b shows the results, when conventional linear analyses and proposed nonlinear analyses, respectively, are performed for the estimation of DRFs. Figure 8c compares the DRFs estimated from linear and nonlinear analyses. Figure 8d compares the nonlinear responses to linear responses. In this comparison, effective period and equivalent damping of the nonlinear systems are used in the linear analysis.

Similar to the uni-directional analyses, significant scatter around the fitted curves are observed. The comparison of the DRFs from the nonlinear analyses provides observations similar to uni-directional case: Equivalent SDOF approach tends to underestimate nonlinear displacement demands of hysteretic systems. Figure 8d helps further to elaborate on the difference between hysteretic systems and the linear systems. The fitted curve of the ratio, which can go up to 1.5, shows an inherent difference between the estimates of displacement of the hysteretic systems and the linear systems with equivalent viscous damping. This difference is not reflected to the DRFs in current literature and considered to be a significant aspect of the proposed method of DRF estimation.

Details of the DRFs based on the GM measure of displacements are not given herein; rather comparison to uni-directional and MR-based DRFs are given in the following section.

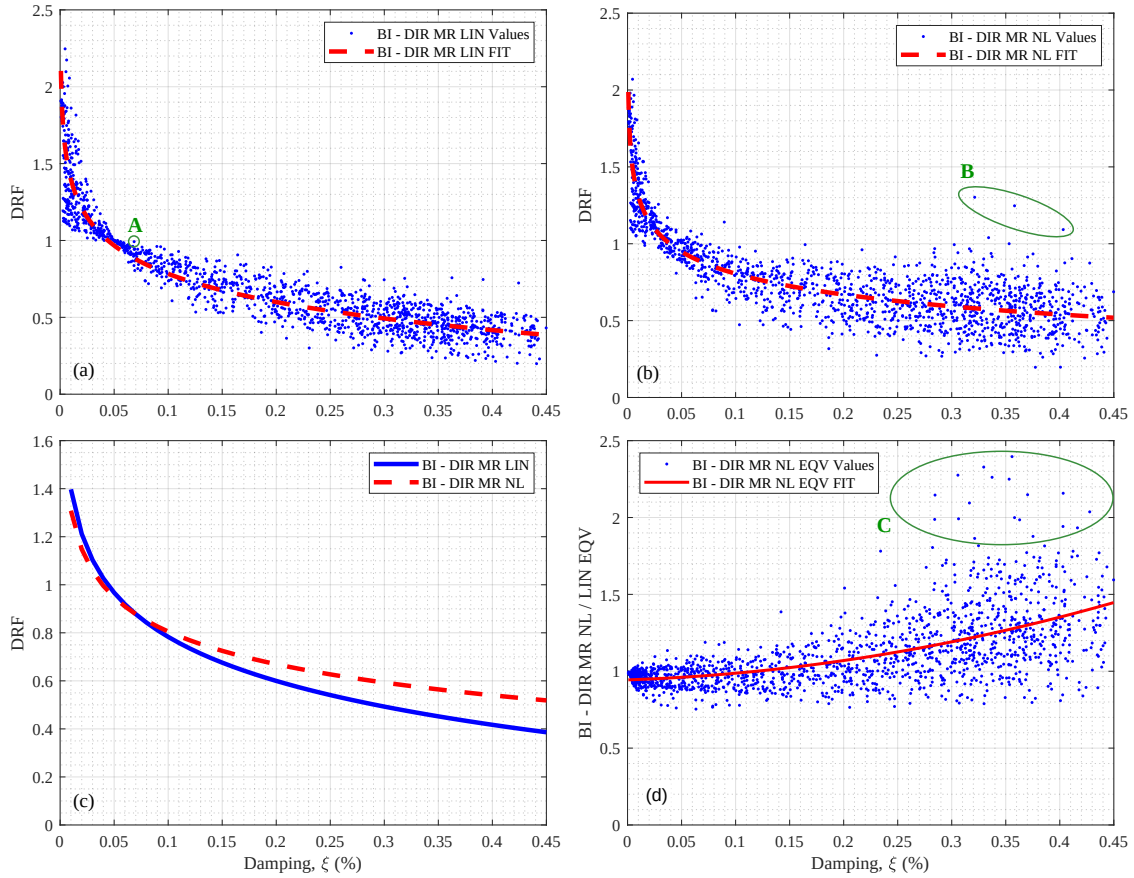

Figure 8. Results for the bi-directional analyses for MR measure (a) linear DRF, (b) nonlinear DRF, (c) linear DRF vs nonlinear DRF and (d) ratio of nonlinear MR displacements to linear MR displacements

4.3. Comparisons of the Results

Figure 9 shows two comparison of the results. Figure 9a shows comparison of DRFs estimated from non-linear analyses for three measures of displacement demands. Further DRFs from the Turkish and American codes and BI-DIR (MR NL) / (GM LIN) DRF are also shown. Comparison of DRFs estimated from linear analyses is not shown here since all plots are same due to linearity of the system and uncoupled behavior in the orthogonal horizontal directions. These plots show that when nonlinear behavior of isolators is reflected to the estimation of DRFs, the isolator displacements will be larger than the case , where conventional DRFs are used. Figure 9b compares the the nonlinear and linear MR DRFs. Further, DRFs from the Turkish and American codes are shown for comparison. Also shown is the plat of BI-DIR (MR NL) / (GM LIN) DRF divided by 1.3, which is a factor given in Turkish code that converts geometric mean displacements to resultant displacements. These plots confirm that, DRFs suitable for base isolation systems (BI-DIR MR NL) yields larger displacements compared to the DRFs suitable for the viscous systems. Also the factor 1.3 given in the Turkish code is an accurate estimate of the ratio of maximum resultant displacements to maximum geometric mean displacements. Directional effects are negligible, possible reason being cancellation of the directional effects during the division.

A large range of isolator properties and a large set of ground motion data are used in this study, which resulted some ratios that are significantly different than the other ratios and best fit curves. Examples of these points are Point A in Figure 8a, Point B in Figure 8b and Point C in Figure 8d. The reason for these behavior explained herein. Point A corresponds to a system with a long effective period (in the order of 4 sec) and ground motion data No. 1166. This specific ground motion data does not result decrease in the displacements due to added viscous damping in the long effective period range. Points B and C correspond to ground motion data No. 900 and No. 1121. These specific ground motions resulted significantly unsymmetrical isolator hystereses, where equivalent viscous damping given by Equation 1 overestimates the hysteretic damping. Therefore, displacement of the hysteretic system is significantly larger than the corresponding equivalent SDOF system.

Table 5. Coefficients of of the DRF curves (see Equation 5)

Figures	a	b	c	Information
ONE-DIR LIN (Figure 7a)	45.815	–0.0057	–45.062	Uni-Dir. Linear DRF
ONE-DIR NL (Figure 7b)	1.462	–0.1037	–1.037	Uni-Dir. Nonlinear DRF
BI-DIR MR LIN (Figure 8a)	48.080	–0.0054	–47.904	Bi-Dir. Maximum Rotated Linear DRF
BI-DIR MR NL (Figure 8b)	2.391	–0.0713	–2.013	Bi-Dir. Maximum Rotated Nonlinear DRF
BI-DIR GM LIN	47.343	–0.0056	–47.175	Bi-Dir. Geometric Mean Linear DRF
BI-DIR GM NL (Figure 9a)	3.521	–0.0529	–3.134	Bi-Dir. Geometric Mean Nonlinear DRF
BI-DIR (MR NL) / (GM LIN) (Figure 9a)	2.874	–0.083	–2.404	DRF suitable for TBEC-18 (2018)

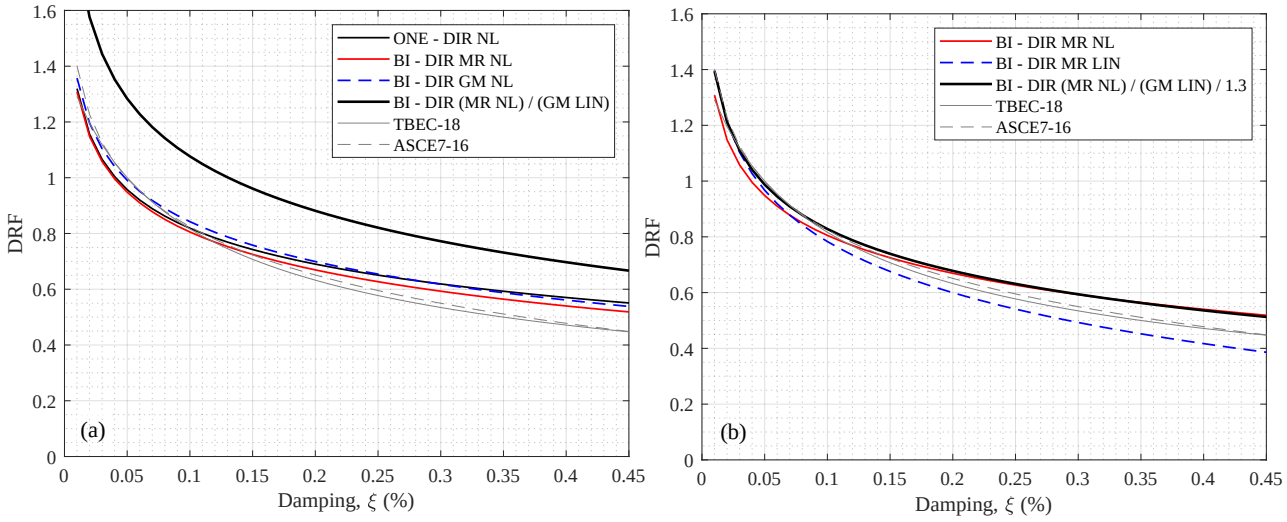

Figure 9. Comparison of DRFs from (a) nonlinear analyses and (b) nonlinear and linear analyses

4.4. Equations of DRF Curves

Suggested DRF curves are obtained by fitting a power-law curve to the data:

$$\beta(\xi) = a\xi^{b} + c \tag{5}$$

where the parameters are obtained using a nonlinear least-squares method (see Table 5).

5. CONCLUSIONS

In this study, damping reduction factors suitable for maximum rotated spectra and base isolation design are investigated. Bilinear model with biaxial interaction in the horizontal directions is used to model isolator behavior and a large set of possible bilinear element parameters is generated. A set of earthquake ground motion is also selected and this set is scaled with several factors in the analyses. Damping reduction factors are proposed to be estimated based on nonlinear analysis and bidirectional measures of the displacement demands. Two measures are used: geometric mean and resultant. Resultant of the response is similar to maximum rotated measure. Damping reduction factors are estimated using conventional and proposed methods. It is shown that use of bidirectional measures given in this paper does not have a significant impact on the damping reduction factors since the bidirectional responses are normalized by another bidirectional responses, while, nonlinear behavior has moderate impact. Damping reduction factors for estimation of isolator resultant displacements for a design spectrum based on geometric mean intensity measure is also given, which is the case for Turkish seismic code. It is shown that the factor 1.3 used in the Turkish code is an accurate estimate for the estimation of resultant demands from geometric spectra.

REFERENCES

Akiyama H (1985). *Earthquake-resistant limit-state design for buildings*. Tokyo, Japan: University of Tokyo Press.

Akkar S, Sandıkkaya MA, and Ay BÖ (2014). "Compatible ground-motion prediction equations for damping scaling factors and vertical-to-horizontal spectral amplitude ratios for the broader Europe region," *Bulletin of Earthquake Engineering*, **12 (1)**: 517–547.

Arakawa T (2012). "A study on damping correction of response spectrum for long period and high damping range". *Proceedings of the 15th World Conference on Earthquake Engineering*. Lisbon, Portugal.

ASCE 7-16 (2016). *Minimum Design Loads and Associated Criteria for Buildings and Other Structures*. ASCE Standard. ASCE/SEI 7-16. Reston, Virginia: American Society of Civil Engineers.

Ashour SA (1987). *Elastic seismic response of buildings with supplemental damping.* PhD thesis. Michigan University.

Bommer JJ, Elnashai AS, and Weir AG (2000). "Compatible acceleration and displacement spectra for seismic design codes". *Proceedings of the 12th World Conference on Earthquake Engineering*. Citeseer: 1–8.

CAL-SEIS-10 (2010). *Caltrans Seismic Design Criteria, Version 1.6*. Sacramento, CA: California Department of Transportation.

Cardone D, Dolce M, and Rivelli M (2009). "Evaluation of reduction factors for high-damping design response spectra," *Bulletin of Earthquake Engineering*, **7 (1)**:p. 273.

Eurocode 8 (2004). *Eurocode 8: Design of Structures for Earthquake Resistance — Part 1: General Rules, Seismic Actions and Rules for Buildings*. Brussels: European Committee For Standardization.

FEMA 440 (2005). *Improvement of Nonlinear Static Seismic Analysis Procedures*. FEMA 440. Washington, D.C.: Fedaral Emergency Management Agency.

GJ50011-10 (2010). *Code for Seismic Design of Buildings*. GJ50011-10. Beijing: China Architecture & Building Press.

Huang WH (2002). *Bi-directional Testing, Modeling, and System Response of Seismically Isolated Bridges*. PhD thesis. Berkeley, CA: University of California, Berkeley.

JP-ISO-01 (2001). *Guidelines for Calculation Procedure and Technical Standard on Seismically Isolated Structures*. Tokyo, Japan: Ministry of Vehicle, Infrastructure and Transport.

Kasai K, Ito H, and Watanabe A (2003). "Peak response prediction rule for a SDOF elasto-plastic system based on equivalent linearization technique," *Journal of Structural Construction Engineering, AIJ*, **571**: 53–62.

Kawashima K and Aizawa K (1986). "Modification of earthquake response spectra with respect to damping ratio". *Proceedings of the 3rd US National Conference on Earthquake Engineering*. Vol. 2: 1107–1116.

Lin YY and Chang KC (2004). "Effects of Site Classes on Damping Reduction Factors," *Journal of Structural Engineering, ASCE*, **130 (11)**: 1667–1675.

Lin YY, Miranda E, and Chang KC (2003). "Study on Damping Reduction Factor for Buildings under Earthquake Ground Motions," *Journal of Structural Engineering*, **129 (2)**: 206–214.

Lin YY, Miranda E, and Chang KC (2005). "Evaluation of damping reduction factors for estimating elastic response of structures with high damping," *Earthquake Engineering & Structural Dynamics*, **34 (11)**: 1427–1443.

Naeim F and Kircher CA (2001). "On the damping adjustment factors for earthquake response spectra," *The Structural Design of Tall Buildings*, **10 (5)**: 361–369.

NCSE-02 (2002). *Seismic-Resistant Construction Standard: General Part and Building*. Madrid, Spain: Ministry of Public Works, Transportation and Environment.

Newmark NM and Hall WJ (1982). *Earthquake Spectra and Design*. Berkeley, CA: Earthquake Enginerieng and Researach Institute.

Newmark NM and Hall WJ (1969). "Seismic design criteria for nuclear reactor facilities". *Proceedings of the 4th World Conf. Earthquake Engineering*: 37–50.

OpenSees (2008). "Open System for Earthquake Engineering Simulation," *Computer Program and Supporting Documentation, Pacific Engineering Research Centre, University of California, Berkeley*,

Priestley MJN, Calvi GM, and Kowalsky MJ (2007). *Displacement-Based Seismic Design of Structures*. Pavia, Italy: IUSS Press.

Ramirez OM, Constantinou MC, Whittaker AS, Kircher CA, and Chrysostomou CZ (2002). "Elastic and Inelastic Seismic Response of Buildings with Damping Systems," *Earthquake Spectra*, **18 (3)**: 531–547.

Rezaeian S, Bozorgnia Y, Idriss IM, Campbell K, Abrahamson N, and Silva W (2012). "Damping scaling of response spectra for shallow crustal earthquakes in active tectonic regions". *Proceedings of the 15th World Conference on Earthquake Engineering*. Lisbon, Portugal.

SAP2000 (2018). *Integrated Software for Structural Ananlysis and Design*. Berkeley, California: Computers and Structures Inc.

Sheikh MN, Tsang HH, Yaghmaei-Sabegh S, and Anbazhagan P (2013). "Evaluation of damping modification factors for seismic response spectra". *Australian Earthquake Engineering Society Conference*. Hobart, Tasmania.

IT-STR-08 (2008). *Approval of the New Technical Standards for Constructions, GU n. 29 4-2-2008- Suppl. Ordinario n. 30*. Rome, Italy: Ministry of the Infrastrutture.

TBEC-18 (2018). *Turkish Building Earthquake Code*. Ankara, Turkey: Ministry of Public Works.

Tolis SV and Faccioli E (1999). "Displacement design spectra," *Journal of Earthquake Engineering*, **3 (01)**: 107–125.

Wu J and Hanson RD (1989). "Study of Inelastic Spectra with High Damping," *Journal of Structural Engineering, ASCE*, **115 (6)**: 1412–1431.

Zhou F, Wenguang L, and Xu Z (2003). "State of the art on applications, R & D and design rules for seismic isolation in China". *Proceedings of the 8th World Seminar on Seismic Isolation, Energy Dissipation and Active Vibration Control of Structures*: 6–10.